Journal of the Saudi Society of Agricultural Sciences (2015) xxx, xxx–xxx

King Saud University

Journal of the Saudi Society of Agricultural Sciences

www.ksu.edu.sa
www.sciencedirect.com

FULL LENGTH ARTICLE

Determining quality and maturity of pomegranates using multispectral imaging

Rasool Khodabakhshian [1], Bagher Emadi [*], Mehdi Khojastehpour, Mahmood Reza Golzarian

Department of Biosystem Engineering, Ferdowsi University of Mashhad, Mashhad, Iran

Received 30 September 2015; accepted 26 October 2015

KEYWORDS

Multispectral imaging;
Maturity;
PLSR;
Pomegranate fruit;
Quality parameters

Abstract In this paper, we investigated the use of multispectral imaging technique to quantify pomegranate fruit quality. Three quality factors including total soluble solids (TSS), pH and firmness were studied at four different maturity stages of 88, 109, 124 and 143 days after full bloom (DAFB) and were correlated with the spectral information extracted from images taken at four wavelength spectra. TSS, pH and firmness of the same samples were recorded using nondestructive methods and then modeled with their corresponding spectral data using partial least squire regression (PLSR). The correlation coefficient (r), RMSEC and RPD for the calibration models was found to be: $r = 0.97$, RMSEC = 0.21 °Brix and RPD = 6.7 °Brix for TSS; $r = 0.93$, RMSEC = 0.035 and RPD = 5.01 for pH; $r = 0.95$, RMSEC = 0.65 N and RPD = 5.65 N for firmness. Also these parameters for the validation models were as follows: $r = 0.97$, RMSEP = 0.22 °Brix and RPD = 5.77 °Brix for TSS; $r = 0.94$, RMSEP = 0.038 and RPD = 4.98 for pH; $r = 0.94$, RMSEP = 0.68 N and RPD = 5.33 N for firmness. The results demonstrated the capability of multispectral imaging and chemometrics as useful techniques to nondestructively monitoring pomegranate main quality attributes.

1. Introduction

Pomegranate is one of important fruits consumed as fresh fruit as well as in processed form such as juice and jams all over the world. Determining optimum ripening stage of pomegranate is important to its use and is related to "technological maturity". Technological maturity mainly corresponds to a number of coordinated physiological and biochemical properties such as firmness, total soluble solids (TSS) and pH (Moing et al., 1998; Opara, 2000; Nunes et al., 2009). Various methods have been used to determine the maturity stages of pomegranate but

* Corresponding author. Tel.: +98 9153007648; fax: +98 511 8787430.
E-mail address: bagher_emadi@yahoo.com (B. Emadi).
[1] Visiting Researcher at Department of Automation, Tsinghua University, Beijing, China.
Peer review under responsibility of King Saud University.

ELSEVIER Production and hosting by Elsevier

http://dx.doi.org/10.1016/j.jssas.2015.10.004

Please cite this article in press as: Khodabakhshian, R. et al., Determining quality and maturity of pomegranates using multispectral imaging. Journal of the Saudi Society of Agricultural Sciences (2015), http://dx.doi.org/10.1016/j.jssas.2015.10.004

most techniques are destructive in nature, time consuming and inapplicable to grading and sorting (Salah and Dilshad, 2002; Al-Said et al., 2009; Zarei et al., 2011; Fawole and Opara, 2013a,b). Therefore, any technology that can classify the fruits non-destructively based on their physiological parameters and nutritional values is of importance and can assure better fruit quality and consistency which in turn increases the consumer acceptance and satisfaction. Many research works have been conducted worldwide to develop nondestructive methods to determine overall quality of pomegranate fruit. Machine vision, NMR, dielectric spectroscopy, and X-ray computed tomography are some of the most recent nondestructive techniques used for quality evaluation of Pomegranate (Blasco et al., 2009; Zhang and McCarthy, 2013; Castro-Giraldez et al., 2013; Magwaza and Opara, 2014).

In light of providing a more consistent and objective evaluation of fruit quality, optical measurement techniques, such as machine vision and Near Infrared (NIR) spectroscopy, are considered as the most potential methods and complementary to the human inspection on the automatic fruit sorting line. Machine vision has been used successfully in categorizing fruits in terms of size, color and other appearance indices. However, its capacity for determination of internal quality parameters is still limited and often not reliable (Lu, 2003; Leemans and Destain, 2004). On the other hand, NIR spectroscopy has been used to evaluate nondestructively the internal quality parameters of many agricultural products (Ying et al., 2005; Guthrie et al., 2006; Shao et al., 2007; Fan et al., 2009). However, since spectroscopy generally measures an aggregate amount of light reflected or transmitted from a specific area of a sample (point measurement), it does not contain spatial information about the product under study.

As an extension of both spectroscopy and imaging techniques, hyperspectral and multispectral imaging techniques have been emerged to integrate both techniques in one system to provide spectral and spatial backgrounds simultaneously. Multispectral imaging, which was originally developed for space-based imaging, may capture light from wavelengths outside of the visible spectral range, such as infrared. It can, therefore, provide more information than what human eye can capture. Multispectral imaging can be used to address features such as ripening (Lu, 2004) and external defects (Diaz et al., 2000, 2004; Kleynen et al., 2003; Leemans and Destain, 2004; Mehl et al., 2004; Unay and Gosselin, 2006) with higher sensitivity in comparison with the ordinary RGB imaging (Aleixos et al., 2002, 2007; Leemans et al., 2002; Kleynen et al., 2003). However, despite an extensive research on multispectral imaging of fruits, yet very limited published results on the multispectral imaging of pomegranate fruit and pomegranate arils are available.

The multispectral imaging is believed to perform as a useful new technique for fruit internal quality evaluation and assessment of postharvest storability. These operations are of interest to growers, breeders and postharvest technologists particularly when implemented non-destructively. Hence, this study was undertaken to acquire the multispectral image of pomegranate fruits at different maturity stages (four distinct maturity stages between 88 and 143 days after full bloom (DAFB)) to model fruits' quality parameters (firmness, TSS and pH) from their multispectral data. The aim was achieved by fulfilling the following specific objectives:

(i) To select the optimal wavelengths that provide the highest correlation between the spectral data and the three studied quality parameters.
(ii) To develop partial least square (PLS) models to quantitatively predict firmness, TSS, and pH in pomegranate fruit, and to examine the prediction accuracy of these models.

2. Material and methods

2.1. Materials

A total of 400 samples for this study were all complete and undamaged pomegranate fruits. The fruits were of *ASHRAF* variety and handpicked from a pomegranate orchard in Shahidabad Village, Behshahr County, Mazandaran Province, Iran (36°41′32″N 53°33′09″E). Harvesting and handpicking started on 31 August 2014, when it was possible to squeeze juice from fruit arils, and ended in October 2014 at fruits' commercially full ripe stage. The 400 sample pomegranates were divided into four groups of 100 samples, each representing maturity levels of 1–4 corresponding to 88, 109, 124 and 143 days after full bloom (DAFB), respectively (Fig. 1). Features of samples at these maturity stages are shown in Table 1. The tested fruits in each maturity stage were randomly divided into two subgroups for training and testing. The first subgroup of 70 samples was used as a training set for developing partial least square (PLS) model. The remaining subgroup of 30 fruits was used for model validation and to verify the prediction power of the models.

2.2. Wavelengths selection

Selecting vital few wavelengths that are most influential on the quality evaluation of the product is often of interest to researchers. They are also interested in eliminating wavelengths having no discrimination power. The selected wavelengths result in data dimensionality reduction while the most important information is preserved in a lower dimensional data space. The responses of the fruits to spectral analysis are considered in determining the selected wavelengths. The main aim of this research also was to select the most suitable wavelength bands based on which we develop a calibration model for predicting quality parameters of pomegranate fruit. Therefore, before acquisition of multispectral images, the whole spectra (400–1100 nm at intervals of 1 nm) of fruit samples were acquired using a dual-channel spectrometer AvaSpec-2048TEC (Avantes Company, Russia) equipped with AvaSoft7 software for Windows, a cooled, one nanometer resolution and sensitivity of 2000 count per 1 mJ entrance irradiation. Then, four most suitable wavelength bands that discriminate studied maturity stages were selected by means of principal component analysis, similar to the approached followed by Miller et al. (1998) and Mehl et al. (2002). PCA is an effective method for data dimensionality reduction and feature extraction. Since each PC is a linear sum of intensity at individual wavelengths multiplied by corresponding spectral weighing coefficients, the wavelengths with weighing coefficients at peaks and valleys represent the dominant wavelengths. The selected wavelengths were as follows: 680, 800, 900, and

Please cite this article in press as: Khodabakhshian, R. et al., Determining quality and maturity of pomegranates using multispectral imaging. Journal of the Saudi Society of Agricultural Sciences (2015), http://dx.doi.org/10.1016/j.jssas.2015.10.004

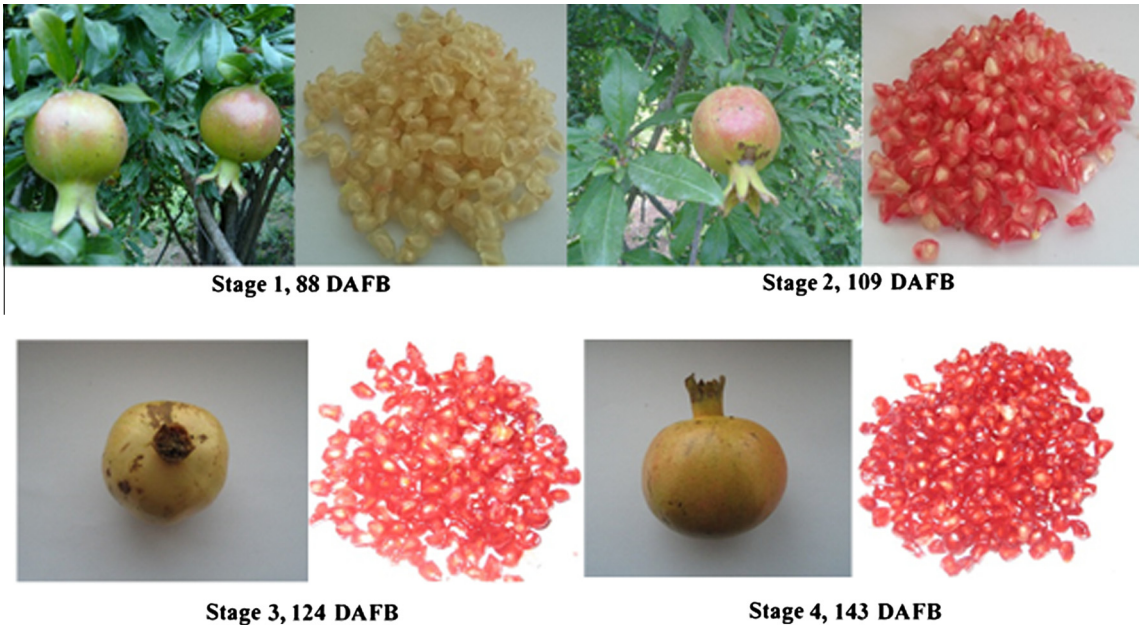

Figure 1 Fruit and arils of pomegranate (*cv.* '*ASHRAF*') cultivar at different maturity stages. Immature stage: 88 DAFB (A); half-ripe stage: 109 DAFB (B) and 124 DAFB (C); and full-ripe stage: 143 DAFB (D).

Table 1 Features of pomegranate fruit samples at four different maturity stages of 88, 109, 124 and 143 days.

Geometrical attributes	Fruit maturity stages (DAFB)			
	S_1 (88)	S_2 (109)	S_3 (124)	S_4 (143)
Length (mm)	47.47^{a} (6.16)	58.86^{b} (1.32)	60.59^{bc} (2.52)	64.02^{c} (2.13)
Width (mm)	48.87^{a} (3.79)	60.17^{b} (2.96)	63.01^{c} (2.12)	70.15^{d} (3.05)
Thickness (mm)	47.80^{a} (4.26)	58.48^{b} (2.74)	62^{b} (3.15)	67.12^{c} (2.6)
Geometric mean diameter (mm)	48.03^{a} (4.76)	59.16^{b} (2.16)	61.85^{b} (2.62)	66.95^{c} (2.13)
Sphericity	0.99^{a} (0.01)	0.98^{a} (0.02)	0.96^{b} (0.01)	0.95^{b} (0.01)
Surface area (mm^2)	7302.35^{a} (1454.37)	11021.15^{b} (827.99)	12017.92^{b} (923.41)	14081.57^{c} (872.13)
Volume (cm^3)	58.05^{a} (5.42)	103.91^{b} (4.94)	123.94^{c} (5.53)	157.20^{d} (6.72)
Mass (g)	63.99^{a} (11.05)	121.55^{b} (8.39)	135^{c} (7.85)	160^{d} (8.12)
True density (g/cm^3)	1.07^{a} (0.19)	1.05^{a} (0.07)	0.944^{a} (0.02)	0.933^{a} (0.23)

Different letter(s) on column indicate statistical significant differences ($p < 0.05$) according to Duncan's multiple range test. n.s = non-significant.

1000 nm. In addition to PCA findings, the selection of these wavelength is supported by the literature having found that 680 nm is related to the absorption of light by chlorophyll in fruit (Abbott et al., 1997; Seeram et al., 2006) and this wavelength was found to be useful for predicting the firmness of apples (Tu et al., 1995; Moons et al., 1997) and the SSC in melons (Sugiyama, 1999). The wavelengths of 880 and 900 nm were also used for predicting SSC in fruits (Slaughter 1995; Moons et al. 1997; Ventura et al., 1998; McGlone and Kawano, 1998; Guthrie and Walsh, 1999). The wavelength of 1000 nm was used for predicting SSC too (Moons et al., 1997).

2.3. Image acquisition

A laboratory multispectral imaging system was developed by authors as shown in Fig. 2. The system is comprised of the following components:

1. A 75(length) × 50(width) × 45(height) cm light chamber that is made of sheet metal.
2. A charged couple device (CCD) camera (SCB-2000, SAMSUNG).
3. An illumination unit that consists of ten 50 W halogen lamps adjusted at angle of 45° to illuminate the camera's field of view.
4. A frame grabber.
5. A filter wheel with four holes for holding filters in place. Three bandpass filters of 800, 900 and 1000 at 25 nm bandwidth (Thorlabs Corp., US) were used. Another space in filter wheel was used with no filter for acquiring RGB images.

2.4. Standard tests of fruit firmness, TSS and pH

After acquisition of multispectral images, each fruit sample was tested for its firmness, TSS and pH. The firmness was

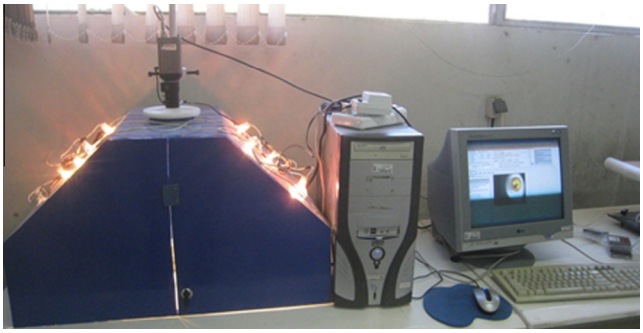

Figure 2 The constructed multispectral imaging system for acquiring images from the fruit.

measured using an Instron Universal Testing Machine (Model H5KS, Tinius Olsen Company, US) with a 5 mm cylindrical probe programmed to penetrate 8 mm into test fruits with a speed of 10 mm/s. Duplicate puncture tests were performed on opposite sides of equatorial region of each fruit and average value was reported. The maximum force required to puncture fruit skin was considered as fruit firmness. For determination of TSS and pH, the fruit samples were juiced with a commercial juice extractor. The juice was filtered and centrifuged afterward. The TSS and pH of juice were measured thrice using a hand-held refractometer (TYM Model, China) and a digital pH meter (3020 Model, GenWay Company, UK) respectively, and the average values of three times measurements were noted and used in the following data analysis section. The juice's TSS, expressed in values of °Brix, was measured following the methods used by many researchers (McGlone et al., 2002; Gomez et al., 2006; Shao et al., 2007; Fawole and Opara, 2013b).

2.5. Image processing and data analyses

2.5.1. Preprocessing of multispectral images

All the acquired multispectral images were processed and analyzed using Matlab (R2013a; Math works Inc, US). The multispectral images were firstly corrected with a white and a dark references. The dark reference was used to remove the effect of dark current of the CCD detectors, which are thermally sensitive. The corrected image (R) was estimated using Eq. (1):

$$R = \frac{R_0 - D}{W - D} \quad (1)$$

where R_0 is the recorded multispectral image, D is the dark reference image (with 0% reflectance) recorded by turning off the lighting source with the lens of the camera completely closed, and W is the white reference image (Teflon whiteboard with 99% reflectance). The corrected images were used as the inputs to the following image analysis. From these images, some information about the spectral properties of each fruit was extracted.

2.5.2. Image processing and recording spectral data

Due to physiological and chemical variations among studied maturity stages of pomegranate fruits, the samples may reflect, absorb, and/or emit electromagnetic energy in distinctive patterns. In essence, these spectral responses can be used to uniquely characterize and identify the studied maturity stages. The following procedure was used to collect the spectral response from samples of each maturity stage. A multispectral maturity classification was proposed based on the ratio of R/IR (red image of sample divided by its corresponding infrared image). Firstly, acquired images at four wavelengths (700, 800, 900 and 1000 nm) from a region of interest (whole fruit region) were selected for the four studied maturity stages (Fig. 3). Then, the spectral ratio images of samples at 700/800, 700/900 and 700/1000 were calculated and compared. To make images of different spectral ratios comparable, the values of each spectral array were normalized by subtracting with minimum value and dividing the product by the "maximum–minimum" difference of each image. After that, the normalized images were converted to grayscale images and the average spectral data of the reigns of interest at each maturity stage were extracted and then converted to absorbance value (Log ($1/R$)). Overall, 400 average spectral data representing 100 samples × 4 maturity stages were recorded and stored for subsequent model development and validation.

2.5.3. Spectral data analysis and building the calibration models

To develop a model between spectral responses from samples and their quality attributes, partial least squares (PLS) regression method was implemented in ParLeS software version 3.1 (ViscarraRossel, 2008). The values of each attribute (firmness, TSS and pH) from the calibration set were used to represent the dependent variables (Y). Meanwhile, the reflectance values at four studied wavelengths from 280 data points (70% of whole data) fruits represented the independent variables or the predictors (X).

The remaining 30% of whole data (from 120 data points) was randomly allocated for validation. The accuracy of the calibration and validation was assessed by correlation coefficient (r), root mean square error of calibration (RMSEC), root mean square error of prediction (RMSEP) and ratio performance deviation (RPD) as follows (Liu et al. 2010):

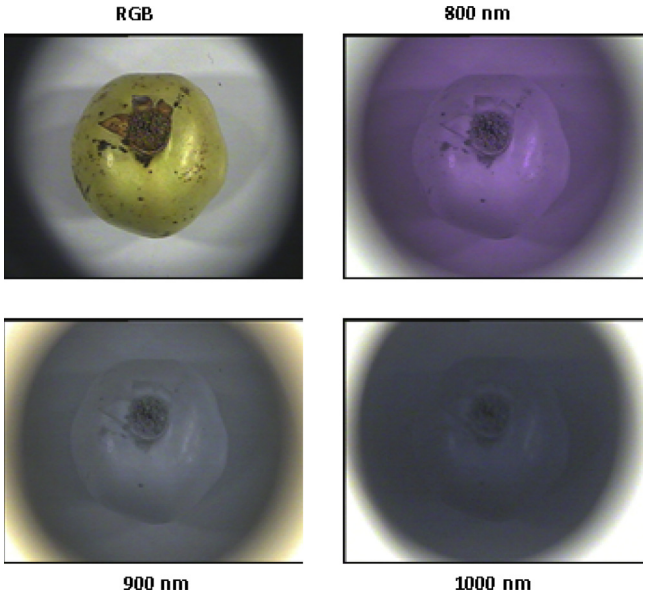

Figure 3 Images of a sample at maturity stage 1 taken at 700, 800, 900 and 1000 nm.

$$r = \sqrt{\sum_{i=1}^{n}(\hat{y}_i - y_i)^2} \Big/ \sqrt{\sum_{i=1}^{n}(\hat{y}_i - y_m)^2} \quad (2)$$

$$\mathrm{RMSEC} = \sqrt{\frac{1}{n_c}\sum_{i=1}^{n_c}(\hat{y}_i - y_i)^2} \quad (3)$$

$$\mathrm{RMSEP} = \sqrt{\frac{1}{n_p}\sum_{i=1}^{n_p}(\hat{y}_i - y_i)^2} \quad (4)$$

$$\mathrm{RPD} = \frac{\mathrm{SD}}{\mathrm{RMSEC(P)}} \quad (5)$$

where $\hat{y}_i$ is the predicted value of the i-th observation, y_i is the measured value of the i-th observation, y_m is the mean value of the calibration or prediction set, n, n_c, and n_p are the total number of observations in the whole data set, in calibration and the number of observations in prediction set, respectively and SD is standard deviation. Generally, a good model should have higher correlation coefficients; lower both RMSEC and RMSEP values, but also a small difference between RMSEC and RMSEP or a RPD value should be more than 5 (Westad et al., 2013).

3. Results and discussion

3.1. Changes in pH, TSS and firmness during maturation

The patterns of how samples' TSSs and pHs change during different maturity stages are presented in Table 2. As shown in this table, TSS and pH increased during the days after DAFB, and they reached to their maximum values of 3.51 and 18.85 °Brix at full ripe stage, respectively. This finding was in agreement with the results found on the same fruit but *Taifi* variety by Salah and Dilshad (2002). Their results showed that fruit's pH and TSS were maximum (and 3.57 and 16.90 °Brix, respectively), at the full-ripe stage. Also Zarei et al. (2011) found that TSS increased significantly during three major fruit developmental stages for pomegranates of '*Rabbab-e-Fars*' cultivar. They found that the TSS content increased from 10.30 °Brix for immature fruits at 20 days after fruit bloom (DAFB) to 19.56 °Brix for fully ripe fruit at 140 DAFS. In addition, findings of Al-Maiman and Ahmad (2002), Kulkarni and Aradhya (2005) and Fawole and Opara (2013a,b) confirm the change pattern of TSS we found in our study. The TSS values obtained by Fawole and Opara (2013a) during the fruit development of pomegranate fruit (Bhagwa cultivar) grown in South Africa, increased by approximately 1.5 times between 54 days after DAFB and commercial harvest at 165 DAFB. Their results were similar to the trend of TSS change in another variety of pomegranate fruit (*Ruby* cultivar).

Table 2 Influence of maturity stages on some quality parameters of '*ASHRAF*' pomegranate cultivar during 2014 growing season.

Property	Fruit maturity stages (DAFB)			
	S_1 (88)	S_2 (109)	S_3 (124)	S_4 (143)
Fruit firmness (N)	50.12	45.12	42.4	40.3
Total soluble solid (°Brix)	15	17.5	18.15	18.85
pH	3.23	3.36	3.42	3.51

The change in firmness also was found to be associated with the stage of maturity. As it is shown in Table 2, the required force to puncture fruit to a depth of 8 mm decreased as the fruit advanced in maturity from S_1 to S_4. It might be due to the changes occurred in the structure of polymers in fruit skins during maturity. Fawole and Opara (2013b) have reported fruit firmness between 123.6 N and 143.6 N during early developmental stages for '*Ruby*' pomegranate cultivars. They found that the force required to puncture fruit to the depth of 8.9 mm decreased significantly during the early stages of maturity. However, they reported that the puncture force increased dramatically as fruits approach their maturity stage.

3.2. Combination of red and near infrared images for classifications purposes

In order to compensate for the geometrical effect of the effect of the fruit, the R/IR ratio was computed and the classification computed following method described in Section 2.5.2. Fig. 4 shows the representations of fruit regions at three different R/IR ratios. Comparing 700/800, 700/900 and 700/1000 images of fruits showed that 700/1000 images had most discrimination between fruits at different maturity stages. Also the average histograms at this ratio were more Gaussian as compared to those obtained with other ratios. Delwiche et al. (1987) investigated color and spectral variations in peaches at various maturity stages. They proposed reflectance

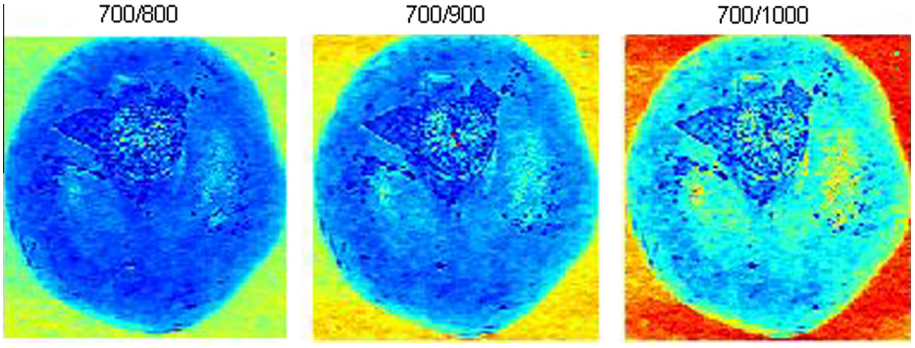

Figure 4 Representations of a sample in ripening stage 1 at wavelength ratios of 700/800, 700/900 and 700/1000.

ratio 670/800 to be a good maturity index for sorting yellow clingstone peaches. Merzlyak et al. (2003) tested the index reflectance ratio 800/678 on apples. They found that this index was linearly related to chlorophyll content in the range 0.4–5 nmol/cm^2, and saturated when chlorophyll exceeded 6 nmol/cm^2. Lleo et al. (2009) proposed *R*/IR histograms to predict ripeness stages of two varieties of peach fruits. They found that as fruits ripened, the associated R/IR histogram skewed to the right with increasing levels of intensity.

3.3. Spectral reflectance

The average reflectance spectra in the range of 700–1000 nm for pomegranate fruit collected at four different maturity levels are shown in Fig. 5. The presence of water in samples gave an increase to the typical absorption bands that seem as localized maxima. The stage containing higher moisture contents (Stage 4) had higher reflectivity across this spectral range. The results of data analysis showed that there was a significant difference

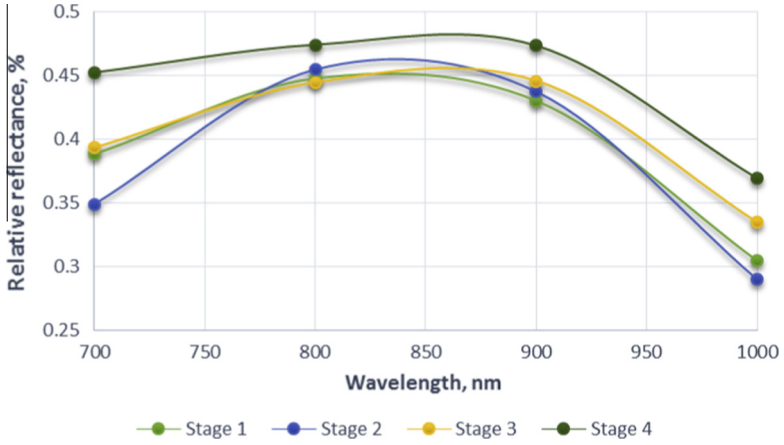

Figure 5 A typical reflectance of VIS/NIR spectrum (700–1000 nm) of pomegranate fruit at different maturity stages.

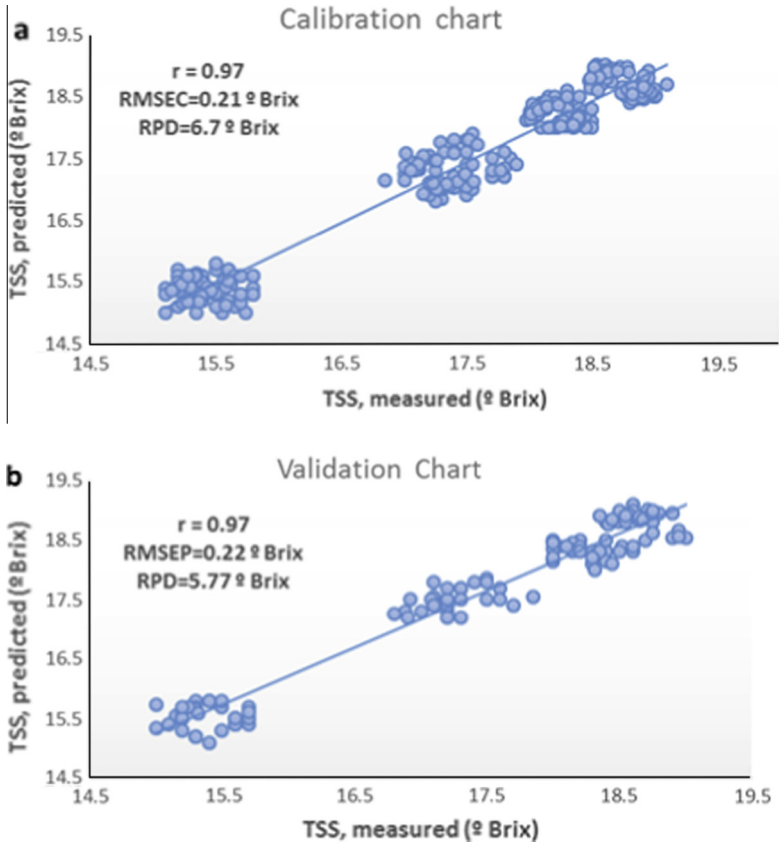

Figure 6 Correlation between measured TSS and estimated TSS for the calibration set (a) and validation set (b) of *ASHRAF* pomegranate fruit.

between reflectance of fruits of four maturity stages. As shown in this figure, a strong distinction was noticed nearly 700 nm which was possibly due to the chlorophyll content in the fruits in their early ripening stage. The absorption regions in the wavelength range of 850–950 nm represent sugars and water absorption bands. The relative reflectance representing sugar absorption bands were higher for the mature fruits (S_3 and S_4) compared to those at their early ripening stages (S_1 and S_2). As the amount of reflectance in spectral band 850–950 nm is also related to the fruit's water content, it can be used to determine fruit's ripening stage based on the amount of moisture available in the fruit. These observed values are similar to the spectral band absorption values reported by Abbott et al. (1997) for apple and Seeram et al. (2006) for strawberry. Since the immature fruit (at maturity stages of S_1 and S_2) peel had lower moisture, consequently, the reflection was also lower in the fruits. The overall difference in reflection spectra of the pomegranate fruits may be due to the noticeable changes that occur simultaneously during maturity such as changes in pH, TSS, and firmness. The results of these changes during maturity are explained and modeled in following sections.

3.4. Prediction of total soluble solids (TSS)

The results of calibration and prediction of PLS models for TSS are shown in Fig. 6. As can be seen the model for prediction of TSS had $r = 0.97$ and RMSEC = 0.21 °Brix (Fig. 6a). The model predicted the TSS of validation samples with $r = 0.97$ and RMSEP of 0.22 °Brix (Fig. 6b). The very high correlation coefficient and low RMSEC indicate that PLS models developed on spectral information have the potential to estimate TSS in pomegranates non-destructively. Zhang and McCarthy (2013) have reported an $r = 0.41$ and RMSECV of 0.57 between measured SSC (Soluble Solid Content) of pomegranate fruit by the reference analytical methods and predicted SSC by NMR from the PLS model. As similar to our findings but on different products, Lu (2004) concluded that the multispectral imaging was found to be a promising technique to determine the soluble solids distribution in apples.

3.5. Prediction of total pH

A good correlation was observed between measured and predicted pH on studied absorption bands. The correlation coefficients (r) for the calibration model were found to be 0.93 and it was 0.94, for validation set (Fig. 7). Also, RMSEC and RMSEP were 0.035 and 0.038, for calibration and evaluation data sets, respectively. Similar to the scatter plot of TSS (Fig. 6), the 45° slope of the line fitted to the pH measured-predicated data points showed that predicted values were very close to measured values (Fig. 7). To the best of our knowledge, there are no any available published results on the use of multispectral imaging and NIR spectroscopy for prediction

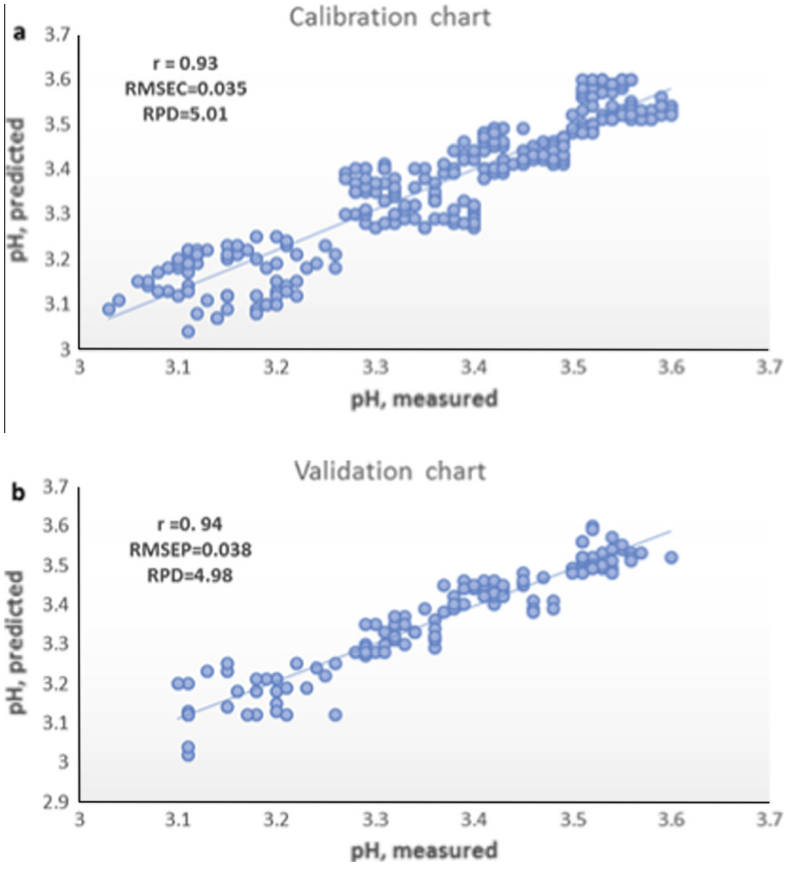

Figure 7 Correlation between measured pH and estimated pH for the calibration set (a) and validation set (b) of *ASHRAF* pomegranate fruit.

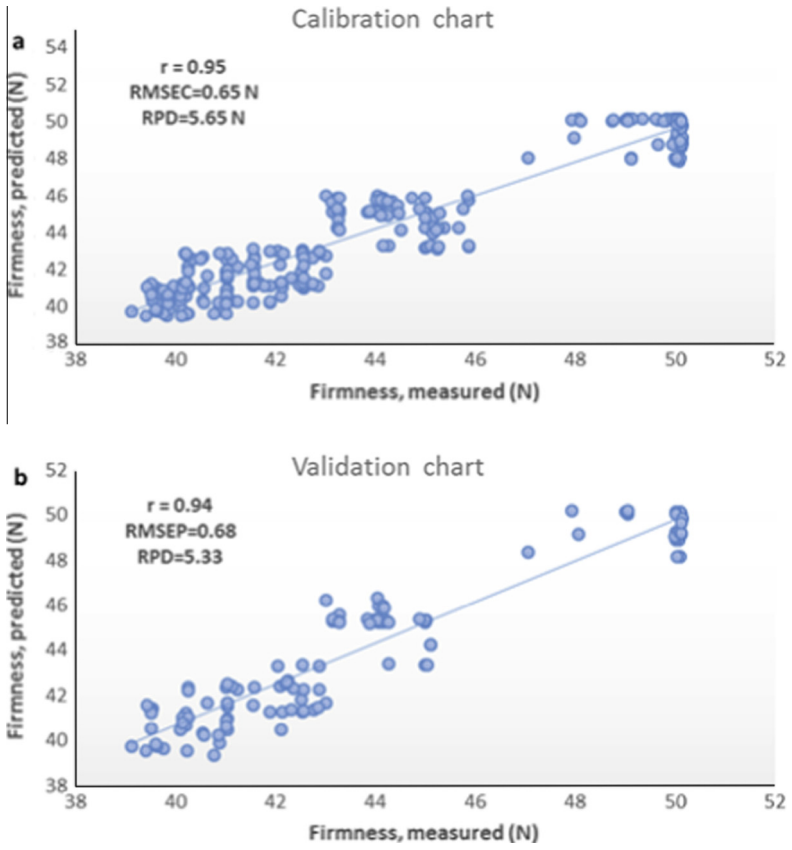

Figure 8 Correlation between measured firmness and estimated firmness for the calibration set (a) and validation set (b) of *ASHRAF* pomegranate fruit.

of pH for pomegranate fruit and arils. However, Zhang and McCarthy (2013) found $r = 0.77$ and RMSECV = 0.13 between measured pH by the reference analytical methods and predicted pH by NMR from the PLS model. They also reported that the RMSECV was very close to RMSEC, which means the loss in the accuracy was very small when the calibration models were applied to the test data. In addition they declared that the low value of the error indicated that the PLS model provided fairly accurate prediction of pH.

3.6. Prediction of firmness

Separate model calibrations and validations were performed for predicting samples' firmness (Fig. 8). The correlation coefficients for the calibration and validation data set of firmness of the pomegranate fruits were found to be 0.95 and 0.94, respectively. The model predicted the firmness of calibration and validation samples with RMSEC and RMSEP of 0.65 N and 0.68 N, respectively. The results showed that predicted values were very close to measured values. The measured firmness was statistically analyzed and presented in Fig. 8. The prediction of firmness is an important textural property of fruit. This property has a direct impact on the fruit's shelf life and consumer acceptance. The fruit firmness is typically influenced by chlorophyll and water content. Despite an extensive research on physical properties of different varieties of pomegranate fruit, very limited published results are available on the mechanical properties (such as firmness) of this fruit and its arils. Lu (2004) concluded that the multispectral imaging was found to be a promising technique to determine the firmness in apples. However, as to pomegranates, to the best of our knowledge, our findings are the first reported results on the prediction of firmness as a mechanical property.

4. Conclusion

In this research PLSR models were developed to relate reflectance spectra obtained from a multispectral imaging system with four wavelengths to the quality parameters of pomegranates during maturity. The results showed that these models could achieve good predictions of TSS, pH and firmness of samples. Therefore multispectral imaging could be used as a nondestructive method to distinguish pomegranate fruit ripening/maturity stages. The correlation coefficient (r), RMSEC and RPD for the calibration models were found to be: $r = 0.97$, RMSEC = 0.21 °Brix and RPD = 6.7 °Brix for TSS; $r = 0.93$, RMSEC = 0.035 and RPD = 5.01 for pH; $r = 0.95$, RMSEC = 0.65 N and RPD = 5.65 N for firmness. Also, these parameters for the validation models were found to be: $r = 0.97$, RMSEP = 0.22 °Brix and RPD = 5.77 °Brix for TSS; $r = 0.94$, RMSEP = 0.038 and RPD = 4.98 for pH; $r = 0.94$, RMSEP = 0.68 N and RPD = 5.33 N for firmness. This information from this study could be used in pomegranate processing industries and also to the biological research centers for implementation of or research on online sorting and grading of pomegranate fruit in terms of quality properties.

Please cite this article in press as: Khodabakhshian, R. et al., Determining quality and maturity of pomegranates using multispectral imaging. Journal of the Saudi Society of Agricultural Sciences (2015), http://dx.doi.org/10.1016/j.jssas.2015.10.004

Conflict of interest

There is no conflict of interest.

Acknowledgment

The authors would like to thank Ferdowsi University of Mashhad for providing the laboratory facilities and financial support (Research Project No. of 28580).

References

Abbott, J.A., Lu, R., Upchurch, B.L., Stroshine, R.L., 1997. Technologies for nondestructive quality evaluation of fruits and vegetables. Hort. Rev. 20 (1), 1–120.

Aleixos, N., Blasco, J., Navarron, F., Molto, E., 2002. Multispectral inspection of citrus in real-time using machine vision and digital signal processors. Comput. Electron. Agric. 33 (2), 121–137.

Aleixos, N., Blasco, J., Gomez, J., Molto, E., 2007. Citrus sorting by identification of the most common defects using multispectral computer vision. J. Food Eng. 83 (3), 384–393.

Al-Maiman, S.A., Ahmad, D., 2002. Changes in physical and chemical properties during pomegranate (Punicagranatum L.) fruit maturation. Food Chem. 76, 437–441.

Al-Said, F.A., Opara, L.U., Al-Yahyai, R.A., 2009. Physico-chemical and textural quality attributes of pomegranate cultivars (Punicagranatum L.) grown in the Sultanate of Oman. J. Food Eng. 90, 129–134.

Blasco, J., Cubero, S., Gomez-Sanchis, J., Mira, P., Molto, E., 2009. Development of a machine for the automatic sorting of pomegranate (Punica granatum) arils based on computer vision. J. Food Eng. 90, 27–34.

Castro-Giraldez, M., Fito, P.J., Ortola, M.D., Balaguer, N., 2013. Study of pomegranate ripening by dielectric spectroscopy. Postharvest Biol. Technol. 86, 346–353.

Delwiche, M., Tang, S., Rumsey, J.W., 1987. Color and optical properties of clingstone peaches related to maturity. Am. Soc. Agric. Eng. 30 (6), 1873–1879.

Diaz, R., Faus, G., Blasco, M., Blasco, J., Molto, E., 2000. The application of a fast algorithm for the classification of olives by machine vision. Food Res. Int. 33 (3–4), 305–309.

Diaz, R., Gil, L., Serrano, C., Blasco, M., Molto, E., Blasco, J., 2004. Comparison of three algorithms in the classification of table olives by means of computer vision. J. Food Eng. 6 (1), 101–107.

Fan, G., Zha, J., Du, R., Gao, L., 2009. Determination of solublesolids and firmness of apples by Vis/NIR transmittance. J. Food Eng. 93, 416–420.

Fawole, O.A., Opara, U.L., 2013a. Changes in physical properties, chemical and elemental composition and antioxidant capacity of pomegranate (cv. 'Ruby') fruit at five maturity stages. Sci. Hort. 150, 37–46.

Fawole, O.A., Opara, U.L., 2013b. Effects of maturity status on biochemical concentration, polyphenol composition and antioxidant capacity of pomegranate fruit arils (cv. 'Bhagwa'). J. S. Afr. Bot. 85, 23–31.

Guthrie, J., Walsh, K., 1999. Influence of environmental and instrumental variables on the non-invasive prediction of Brix in pineapple using near infrared spectroscopy. Aust. J. Exp. Agric. 39, 73–80.

Guthrie, J.A., Liebenberg, C.J., Walsh, K.B., 2006. NIR model development and robustness in prediction of melon fruit total soluble solids. Aust. J. Exp. Agric. 57, 1–8.

Kleynen, O., Leemans, V., Destain, M.F., 2003. Selection of the most efficient wavelength bands for 'Jonagold' apple sorting. Postharvest Biol. Technol. 30 (3), 221–232.

Kulkarni, A.P., Aradhya, S.M., 2005. Chemical changes and antioxidant activity in pomegranate arils during fruit development. Food Chem. 93, 319–324.

Leemans, V., Magein, H., Destain, M.F., 2002. AE – automation and emerging technologies: on-line fruit grading according to their external quality using machine vision. Biosyst. Eng. 83 (4), 397–404.

Leemans, V., Destain, M.F., 2004. A real-time grading method of apples based on features extracted from defects. J. Food Eng. 61, 83–89.

Liu, F., Wang, L., He, Y., 2010a. Application of effective wavelengths for variety identification of instant milk teas. J. Zhejiang Univ. 44, 619–623.

Liu, Y.D., Sun, X.D., Ouyang, A.G., 2010b. Nondestructive measurement of soluble solid content of navel orange fruit by visible–NIR spectrometric technique with PLSR and PCA-BPNN. LWT – Food Sci. Technol. 43, 602–607.

Lleo, L., Barreiro, P., Ruiz-Altisent, M., Herrero, A., 2009. Multispectral images of peach related to firmness and maturity at harvest. J. Food Eng. 93 (2), 229–235.

Lu, R., 2003. Detection of bruises on apples using near-infrared hyperspectral imaging. Trans. ASAE 46, 523–530.

Lu, R., 2004. Multispectral imaging for predicting firmness and soluble solids content of apple fruit. Postharvest Biol. Technol. 31 (2), 147–157.

Magwaza, L.S., Opara, U.L., 2014. Investigating non-destructive quantification and characterization of pomegranate fruit internal structure using X-ray computed tomography. Postharvest Biol. Technol. 95, 1–6.

McGlone, V.A., Kawano, S., 1998. Firmness, dry-matter and soluble-solids assessment of postharvest kiwifruit by NIR spectroscopy. Postharvest Biol. Technol. 13, 131–141.

Mehl, P.M., Chao, K., Kim, M., Chen, Y.R., 2002. Detection of defects on selected apple cultivars using hyper spectral and multispectral image analysis. Appl. Eng. Agric. 18, 219–226.

Mehl, P.M., Chen, Y.R., Kim, S., Chan, D.E., 2004. Defect and contamination detection and fruit classification: development of hyperspectral imaging technique for the detection of apple surface defects and contaminations. J. Food Eng. 61 (1), 67–81.

Merzlyak, M.N., Solovchenko, A.E., Gitelson, A.A., 2003. Reflectance spectral features and non-destructive estimation of chlorophyll, carotenoid and anthocyanin content in apple fruit. Postharvest Biol. Technol. 27 (2), 197–211.

Miller, W.M., Throop, J.A., Upchurch, B.L., 1998. Pattern recognition models for spectral reflectance evaluation of apple blemishes. Postharvest Biol. Technol. 14, 11–20.

Moing, A., Svanella, L., Rolin, D., Gaudillère, M., Gaudillère, J.P., Monet, R., 1998. Compositional changes during the fruit development of two peach cultivars differing in juice acidity. J. Am. Soc. Hort. Sci. 123, 770–775.

Moons, E., Dardenne, P., Dubois, A., Sindic, M., 1997. Nondestructive visible and NIR spectroscopy measurement for the determination of apple internal quality. Acta Hort. 517, 441–448.

Nunes, C., Rato, A.E., Barros, A.S., Saraiva, J.A., Coimbra, M.A., 2009. Search for suitable maturation parameters to define the harvest maturity of plums (Prunusdomestica L.): a case study of candied plums. Food Chem. 112, 570–574.

Opara, L.U., 2000. Fruit growth measurement and analysis. Hort. Rev. 24, 373–431.

Salah, A.A., Dilshad, A., 2002. Changes in physical and chemical properties during pomegranate (Punicagranatum L.) fruit maturation. Food Chem. 76, 437–441.

Seeram, N.P., Lee, R., Scheuller, H.S., Heber, D., 2006. Identification of phenolic compounds in strawberries by liquid chromatography electrospray ionization mass spectroscopy. Food Chem. 97 (1), 1–11.

Shao, Y., He, Y., Gomez, A.H., Pereir, A.G., Qiu, Z., Zhag, Y., 2007. Visible/near infrared spectrometric technique for nondestructive assessment of tomato 'Heatwave' (Lycopersicumesculentum) quality characteristics. J. Food Eng. 81, 672–678.

Slaughter, D.C., 1995. Nondestructive determination of internal quality in peaches and nectarines. Am. Soc. Agric. Eng. 38 (2), 617–623.

Sugiyama, J., 1999. Visualization of sugar content in the flesh of a melong by near-infrared imaging. J. Agric. Food Chem. 47, 2715–2718.

Tu, K., De Busscher, R., De Baerdemaeker, J., Schrevens, E, 1995. Using laser beam as light source to study tomato and apple quality non-destructively. In: Proceeding of the Food Processing Automation IV Conference, 3–5 November, Chicago, IL, pp. 528–536.

Unay, D., Gosselin, B., 2006. Automatic defect segmentation of 'Jonagold' apples on multi-spectral images: a comparative study. Postharvest Biol. Technol. 42 (3), 271–279.

Ventura, M., de Jager, A., De Putter, H., Roelofs, F.P.M.M., 1998. Non-destructive determination of soluble solids in apple fruit by near infrared spectroscopy (NIRS). Postharvest Biol. Technol. 14 (1), 21–27.

ViscarraRossel, R.A., 2008. ParLeS: software for chemometric analysis of spectroscopic data. Chemomet. Intell. Lab. Syst. 90, 72–83.

Westad, F., Bevilacqua, M., Marini, F., 2013. Regression. In: Marini, F. (Ed.), Chemometrics in Food Chemistry. ELSEVIER, Amsterdam: Netherlands, pp. 127–169.

Ying, Y.B., Liu, Y.D., Wang, J.P., Fu, X.P., Li, Y.B., 2005. Fourier transform near-infrared determination of total soluble solids and available acid in intact peaches. Trans. ASAE 48, 229–234.

Zarei, M., Azizi, M., Bashir-Sadr, Z., 2011. Evaluation of physicochemical characteristics of pomegranate (Punicagranatum L.) fruit during ripening. Fruits 66, 121–129.

Zhang, L., McCarthy, M.J., 2013. Assessment of pomegranate postharvest quality using nuclear magnetic resonance. Postharvest Biol. Technol. 77, 59–66.

Please cite this article in press as: Khodabakhshian, R. et al., Determining quality and maturity of pomegranates using multispectral imaging. Journal of the Saudi Society of Agricultural Sciences (2015), http://dx.doi.org/10.1016/j.jssas.2015.10.004